

# Renormalization group analysis of the QCD quark potential to order $v^2$

Aneesh V. Manohar\* and Iain W. Stewart†

Department of Physics, University of California at San Diego,  
9500 Gilman Drive, La Jolla, CA 92099

## Abstract

A one-loop renormalization group analysis of the order  $v^2$  relativistic corrections to the static QCD potential is presented. The velocity renormalization group is used to simultaneously sum  $\ln(m/mv)$  and  $\ln(m/mv^2)$  terms. The results are compared to previous calculations in the literature.

Typeset using REVTeX

---

\*amanohar@ucsd.edu

†iain@schwinger.ucsd.edu

The quark-antiquark interaction potential is needed to compute properties of heavy quark systems, such as  $\Upsilon$  mesons, or  $t\bar{t}$  production near threshold. In this paper, we will study the renormalization group improved potential at one-loop. The calculation makes use of NRQCD, formulated as an effective theory with an expansion in the velocity,  $v$  [1–13]. The leading order term in  $v$  is the Coulomb potential, which has been computed to two-loop order [14,15] using QCD perturbation theory. The renormalization group running of this term is given by the QCD  $\beta$ -function, as is well-known. We will compute the one-loop running of the order  $v$  and  $v^2$  corrections to the quark potential, using a formulation of NRQCD introduced recently [16], and assuming  $mv^2 \gg \Lambda_{\text{QCD}}$ . In QCD the one-loop potential to order  $v^2$  has been computed previously [17,18]. For  $\mu = m$  the logarithms in the effective theory must agree with the logarithmic terms in these computations. We find agreement when some previously neglected terms are included in the spin-independent part of the quark potential. The renormalization group analysis allows one to resum logarithms of  $v$  in the effective theory, which is not possible using only the one-loop quark potential.

The formalism we will use has been described in Ref. [16], and will be called vNRQCD.<sup>1</sup> In vNRQCD, one matches onto QCD at  $\mu = m$  and then runs to lower scales in the effective theory using a velocity renormalization group (VRG). The VRG allows one to simultaneously sum logarithms of  $mv$  and  $mv^2$  in the effective theory. In an alternative approach, called pNRQCD [8], the matching takes place in two stages, at  $\mu = m$  and then at  $\mu = mv$ . The logarithmic corrections to the potential were recently computed using pNRQCD by Brambilla et al. [19]. Our results agree with theirs when the resummed logarithms are expanded to linear order.

The vNRQCD effective Lagrangian is written in terms of fields  $\psi_{\mathbf{p}}$  which annihilate a quark,  $\chi_{\mathbf{p}}$  which annihilate an antiquark,  $A_{\mathbf{p}}^{\mu}$  which annihilate and create soft gluons, and  $A^{\mu}$  which annihilate and create ultrasoft gluons. The covariant derivative is  $D^{\mu} = \partial^{\mu} + igA^{\mu} = (D^0, -\mathbf{D})$ , so that  $D^0 = \partial^0 + igA^0$ ,  $\mathbf{D} = \nabla - ig\mathbf{A}$ , and involves only the ultrasoft gluon fields. The ultrasoft piece of the effective Lagrangian we need contains the quark, antiquark, and ultrasoft gluon kinetic energies,

$$\begin{aligned} \mathcal{L}_u = & -\frac{1}{4}F^{\mu\nu}F_{\mu\nu} + \sum_{\mathbf{p}} \psi_{\mathbf{p}}^{\dagger} \left\{ iD^0 - \frac{(\mathbf{p} - i\mathbf{D})^2}{2m} + \frac{\mathbf{p}^4}{8m^3} \right\} \psi_{\mathbf{p}} \\ & + \chi_{\mathbf{p}}^{\dagger} \left\{ iD^0 - \frac{(\mathbf{p} - i\mathbf{D})^2}{2m} + \frac{\mathbf{p}^4}{8m^3} \right\} \chi_{\mathbf{p}}, \end{aligned} \quad (1)$$

where the covariant derivative on  $\psi_{\mathbf{p}}$  and  $\chi_{\mathbf{p}}$  contain the color matrices  $T^A$  and  $\bar{T}^A$  for the  $\mathbf{3}$  and  $\bar{\mathbf{3}}$  representations, respectively. The coefficients in Eq. (1) do not run due to reparameterization invariance [20]. The potential interaction is

$$\mathcal{L}_p = -V_{\alpha\beta\lambda\tau}(\mathbf{p}, \mathbf{p}') \psi_{\mathbf{p}'}^{\dagger}_{\alpha} \psi_{\mathbf{p}\beta} \chi_{-\mathbf{p}'}^{\dagger}_{\lambda} \chi_{-\mathbf{p}\tau}, \quad (2)$$

where  $\alpha, \beta, \lambda, \tau$  denote color and spin indices. It is convenient to write the terms in  $V$  in matrix form. For example,

---

<sup>1</sup>Following a suggestion of A.H. Hoang.

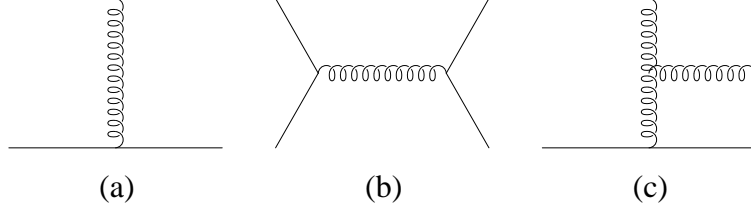


FIG. 1. QCD diagrams for tree level matching.

$$V = \frac{4\pi\alpha_s}{(\mathbf{p} - \mathbf{p}')^2} (T^A \otimes \bar{T}^A) \quad (3)$$

represents the Coulomb interaction, and corresponds to Eq. (2) with

$$V_{\alpha\beta\lambda\tau}(\mathbf{p}, \mathbf{p}') = \frac{4\pi\alpha_s}{(\mathbf{p} - \mathbf{p}')^2} T_{\alpha\beta}^A \bar{T}_{\lambda\tau}^A. \quad (4)$$

The diagrams in Fig. 1a,b give terms of the form

$$V = (T^A \otimes \bar{T}^A) \left[ \frac{\mathcal{V}_c^{(T)}}{\mathbf{k}^2} + \frac{\mathcal{V}_r^{(T)}(\mathbf{p}^2 + \mathbf{p}'^2)}{2m^2 \mathbf{k}^2} + \frac{\mathcal{V}_s^{(T)}}{m^2} \mathbf{S}^2 + \frac{\mathcal{V}_\Lambda^{(T)}}{m^2} \Lambda(\mathbf{p}', \mathbf{p}) + \frac{\mathcal{V}_t^{(T)}}{m^2} T(\mathbf{k}) \right] \\ + (1 \otimes 1) \frac{\mathcal{V}_s^{(1)}}{m^2} \mathbf{S}^2, \quad (5)$$

where  $\mathbf{k} = \mathbf{p}' - \mathbf{p}$  and the notation of Titard and Yndurain [18] has been used:

$$\mathbf{S} = \frac{\boldsymbol{\sigma}_1 + \boldsymbol{\sigma}_2}{2}, \quad \Lambda(\mathbf{p}', \mathbf{p}) = -i \frac{\mathbf{S} \cdot (\mathbf{p}' \times \mathbf{p})}{\mathbf{k}^2}, \quad T(\mathbf{k}) = \boldsymbol{\sigma}_1 \cdot \boldsymbol{\sigma}_2 - \frac{3 \mathbf{k} \cdot \boldsymbol{\sigma}_1 \mathbf{k} \cdot \boldsymbol{\sigma}_2}{\mathbf{k}^2}. \quad (6)$$

The terms with coefficients  $\mathcal{V}_c^{(T)}$ ,  $\mathcal{V}_s^{(T,1)}$ ,  $\mathcal{V}_\Lambda^{(T)}$ , and  $\mathcal{V}_t^{(T)}$  are order  $v^2$  corrections to the lowest order Coulomb term,  $\mathcal{V}_c^{(T)}$ . Matching to the tree level diagram in Fig. 1a at  $\mu = m$  gives

$$\mathcal{V}_c^{(T)} = 4\pi\alpha_s(m), \quad \mathcal{V}_r^{(T)} = 4\pi\alpha_s(m), \quad \mathcal{V}_s^{(T)} = -\frac{4\pi\alpha_s(m)}{3}, \\ \mathcal{V}_\Lambda^{(T)} = -6\pi\alpha_s(m), \quad \mathcal{V}_t^{(T)} = -\frac{\pi\alpha_s(m)}{3}, \quad \mathcal{V}_s^{(1)} = 0. \quad (7)$$

The annihilation diagram in Fig. 1b gives the additional contributions

$$\mathcal{V}_{s,a}^{(T)} = \frac{1}{N_c} \pi \alpha_s(m), \quad \mathcal{V}_{s,a}^{(1)} = \frac{(N_c^2 - 1)}{2N_c^2} \pi \alpha_s(m). \quad (8)$$

These contributions have been separated from those in Eq. (7) to facilitate comparison with results in the literature. In the color singlet channel there is no annihilation contribution.

We have chosen to use the basis in which the potential  $V$  is written as a linear combination of  $1 \otimes 1$  and  $T \otimes \bar{T}$ . One can convert to the singlet and octet potential, using the linear transformation

$$\begin{bmatrix} V_{\text{singlet}} \\ V_{\text{octet}} \end{bmatrix} = \begin{bmatrix} 1 & -C_F \\ 1 & \frac{1}{2}C_A - C_F \end{bmatrix} \begin{bmatrix} V_{1 \otimes 1} \\ V_{T \otimes T} \end{bmatrix}, \quad (9)$$

where  $C_F = (N_c^2 - 1)/(2N_c)$  and  $C_A = N_c$ .

Potential terms can also be induced by operator mixing in the renormalization group flow. For instance, we will see that the running at one-loop induces order  $v^2$  terms of the form

$$V = (T^A \otimes \bar{T}^A) \frac{\mathcal{V}_2^{(T)}}{m^2} + (1 \otimes 1) \frac{\mathcal{V}_2^{(1)}}{m^2}, \quad (10)$$

which are absent at tree level. Additional terms also occur when matching the potential at higher orders in the loop expansion. For instance, at one loop the order  $v$  correction

$$V_{\text{singlet}} = \frac{\mathcal{V}_k^{(s)} \pi^2}{m |\mathbf{k}|} \quad (11)$$

is generated. Ref. [18] has  $\mathcal{V}_k^{(s)} = -C_F(C_A - C_F/2) \alpha_s(m)^2$  for the matching at  $\mu = m$ .

There are terms in the Lagrangian where ultrasoft gluons couple to potential operators. For instance, the diagram in Fig. 1c generates the term

$$\mathcal{L}_{pu} = \frac{2ig^2}{(\mathbf{p}' - \mathbf{p})^4} f^{ABC} (\mathbf{p} - \mathbf{p}') \cdot (g\mathbf{A}^C) [\psi_{\mathbf{p}'}^\dagger T^A \psi_{\mathbf{p}} \chi_{-\mathbf{p}'}^\dagger \bar{T}^B \chi_{-\mathbf{p}}]. \quad (12)$$

The terms in the soft Lagrangian that we need for our computation are

$$\begin{aligned} \mathcal{L}_s = \sum_q \left\{ \left| q^\mu A_q^\nu - q^\nu A_q^\mu \right|^2 + \bar{\varphi}_q \not{D} \varphi_q + \bar{c}_q q^2 c_q \right\} \\ - g^2 \sum_{\mathbf{p}, \mathbf{p}', q, q'} \left\{ \frac{1}{2} \psi_{\mathbf{p}'}^\dagger [A_{q'}^\mu, A_q^\nu] U_{\mu\nu}^{(\sigma)} \psi_{\mathbf{p}} + \frac{1}{2} \psi_{\mathbf{p}'}^\dagger \{A_{q'}^\mu, A_q^\nu\} W_{\mu\nu}^{(\sigma)} \psi_{\mathbf{p}} \right. \\ \left. + \psi_{\mathbf{p}'}^\dagger [\bar{c}_{q'}, c_q] Y^{(\sigma)} \psi_{\mathbf{p}} + (\psi_{\mathbf{p}'}^\dagger T^B Z_\mu^{(\sigma)} \psi_{\mathbf{p}}) (\bar{\varphi}_{q'} \gamma^\mu T^B \varphi_q) \right\} + (\psi \rightarrow \chi, T \rightarrow \bar{T}). \end{aligned} \quad (13)$$

Here  $U$ ,  $W$ ,  $Y$ , and  $Z$  are functions of  $(\mathbf{p}, \mathbf{p}', q, q')$  and matrices in spin and are generated by integrating out the intermediate offshell quarks and gluons in Fig. 2. The field  $c_q$  is the soft ghost field, and  $\varphi_q$  is the massless soft quark field with  $n_f$  flavor components. The index  $\sigma$  denotes the relative order in the  $v$  expansion. Performing the matching in Fig. 2 in Feynman gauge we find

$$\begin{aligned} U_{00}^{(0)} &= \frac{1}{q^0}, \quad U_{0i}^{(0)} = -\frac{(2\mathbf{p}' - 2\mathbf{p} - \mathbf{q})^i}{(\mathbf{p}' - \mathbf{p})^2}, \quad U_{i0}^{(0)} = -\frac{(\mathbf{p} - \mathbf{p}' - \mathbf{q})^i}{(\mathbf{p}' - \mathbf{p})^2}, \quad U_{ij}^{(0)} = \frac{-2q^0 \delta^{ij}}{(\mathbf{p}' - \mathbf{p})^2}, \\ U_{00}^{(1)} &= \frac{(\mathbf{p}' + \mathbf{p}) \cdot \mathbf{q}}{2m(q^0)^2} - \frac{(\mathbf{p}' + \mathbf{p}) \cdot \mathbf{q}}{m(\mathbf{p}' - \mathbf{p})^2} - \frac{ic_F \boldsymbol{\sigma} \cdot [\mathbf{q} \times (\mathbf{p} - \mathbf{p}')] }{m(\mathbf{p}' - \mathbf{p})^2}, \\ U_{0i}^{(1)} &= -\frac{(\mathbf{p} + \mathbf{p}')^i}{2mq^0} + \frac{ic_F(\mathbf{q} \times \boldsymbol{\sigma})^i}{2mq^0} + \frac{q^0(\mathbf{p} + \mathbf{p}')^i}{2m(\mathbf{p}' - \mathbf{p})^2} + \frac{ic_F q^0[(\mathbf{p} - \mathbf{p}') \times \boldsymbol{\sigma}]^i}{2m(\mathbf{p}' - \mathbf{p})^2}, \\ U_{i0}^{(1)} &= -\frac{(\mathbf{p} + \mathbf{p}')^i}{2mq^0} - \frac{ic_F[(\mathbf{p} - \mathbf{p}' + \mathbf{q}) \times \boldsymbol{\sigma}]^i}{2mq^0} + \frac{q^0(\mathbf{p} + \mathbf{p}')^i}{2m(\mathbf{p}' - \mathbf{p})^2} + \frac{ic_F q^0[(\mathbf{p} - \mathbf{p}') \times \boldsymbol{\sigma}]^i}{2m(\mathbf{p}' - \mathbf{p})^2}, \end{aligned} \quad (14)$$

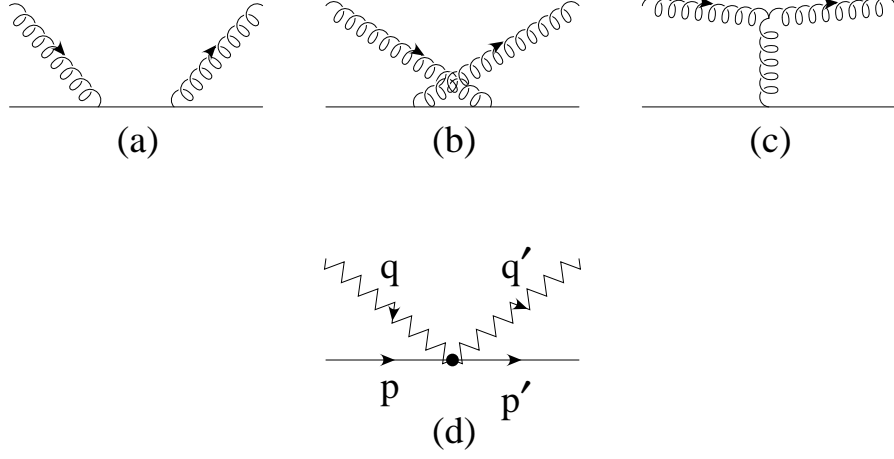


FIG. 2. The Compton scattering diagrams (a,b,c) generate the soft gluon coupling (d) in the effective theory. Diagrams analogous to (c) but with external ghosts or massless quarks generate the soft ghost and massless soft quark couplings in Eq. (13).

$$\begin{aligned}
U_{ij}^{(1)} &= \frac{ic_F \epsilon^{ijk} \boldsymbol{\sigma}^k}{2m} + [2\delta^{ij} \mathbf{q}^m + \delta^{im} (2\mathbf{p}' - 2\mathbf{p} - \mathbf{q})^j + \delta^{jm} (\mathbf{p} - \mathbf{p}' - \mathbf{q})^i] \\
&\quad \times \left[ \frac{(\mathbf{p} + \mathbf{p}')^m + ic_F \epsilon^{mkl} (\mathbf{p} - \mathbf{p}')^k \boldsymbol{\sigma}^l}{2m(\mathbf{p}' - \mathbf{p})^2} \right], \\
U_{00}^{(2)} &= -\frac{c_D (\mathbf{p}' - \mathbf{p})^2}{8m^2 q^0} + \frac{c_S i\boldsymbol{\sigma} \cdot (\mathbf{p}' \times \mathbf{p})}{4m^2 q^0} + \frac{(\mathbf{p} \cdot \mathbf{q})^2 + (\mathbf{p}' \cdot \mathbf{q})^2}{2m^2 (q^0)^3} + \frac{(2 - c_D)(\mathbf{p} - \mathbf{p}') \cdot \mathbf{q}}{4m^2 q^0} \\
&\quad + \frac{(1 - c_D) \mathbf{q}^2}{4m^2 q^0}, \\
U_{0i}^{(2)} &= -\frac{[\mathbf{p} \cdot \mathbf{q} (2\mathbf{p} + \mathbf{q})^i + \mathbf{p}' \cdot \mathbf{q} (2\mathbf{p}' - \mathbf{q})^i]}{4m^2 (q^0)^2} + \frac{ic_F [\mathbf{q} \times \boldsymbol{\sigma}]^i (\mathbf{p} + \mathbf{p}') \cdot \mathbf{q}}{4m^2 (q^0)^2} \\
&\quad + \frac{(c_D - 1)(\mathbf{p} - \mathbf{p}' + \mathbf{q})^i}{4m^2} + \frac{(2\mathbf{p}' - 2\mathbf{p} - \mathbf{q})^i}{4m^2} \left[ \frac{c_D}{2} - \frac{c_S i\boldsymbol{\sigma} \cdot (\mathbf{p}' \times \mathbf{p})}{(\mathbf{p}' - \mathbf{p})^2} \right], \\
U_{i0}^{(2)} &= -\frac{[\mathbf{p} \cdot \mathbf{q} (\mathbf{p} + \mathbf{p}' + \mathbf{q})^i + \mathbf{p}' \cdot \mathbf{q} (\mathbf{p} + \mathbf{p}' - \mathbf{q})^i]}{4m^2 (q^0)^2} - \frac{ic_F [(\mathbf{p} - \mathbf{p}' + \mathbf{q}) \times \boldsymbol{\sigma}]^i (\mathbf{p} + \mathbf{p}') \cdot \mathbf{q}}{4m^2 (q^0)^2} \\
&\quad + \frac{(c_D - 1) \mathbf{q}^i}{4m^2} + \frac{(\mathbf{p} - \mathbf{p}' - \mathbf{q})^i}{4m^2} \left[ \frac{c_D}{2} - \frac{c_S i\boldsymbol{\sigma} \cdot (\mathbf{p}' \times \mathbf{p})}{(\mathbf{p}' - \mathbf{p})^2} \right], \\
U_{ij}^{(2)} &= \frac{(\mathbf{p} + \mathbf{p}')^i (\mathbf{p} + \mathbf{p}')^j}{4m^2 q^0} + \frac{c_F^2 (\mathbf{p} - \mathbf{p}') \cdot \mathbf{q} \delta^{ij}}{4m^2 q^0} + \frac{ic_F (\mathbf{p} + \mathbf{p}')^j [(\mathbf{p} - \mathbf{p}') \times \boldsymbol{\sigma}]^i}{4m^2 q^0} \\
&\quad - \frac{ic_F \epsilon^{ijk} \mathbf{q}^k \boldsymbol{\sigma} \cdot (\mathbf{p} + \mathbf{p}')}{4m^2 q^0} + \frac{ic_F \epsilon^{ijk} \boldsymbol{\sigma}^k (\mathbf{p} + \mathbf{p}') \cdot \mathbf{q}}{4m^2 q^0} + \frac{(1 - c_F^2) \mathbf{q}^i (\mathbf{p} - \mathbf{p}' + \mathbf{q})^j}{4m^2 q^0} \\
&\quad + \frac{(c_F^2 - c_D) \mathbf{q}^2 \delta^{ij}}{4m^2 q^0} + \frac{\delta^{ij} q^0}{2m^2} \left[ \frac{c_D}{2} - \frac{c_S i\boldsymbol{\sigma} \cdot (\mathbf{p}' \times \mathbf{p})}{(\mathbf{p}' - \mathbf{p})^2} \right],
\end{aligned}$$

$$\begin{aligned}
W_{\mu\nu}^{(0)} &= 0, \\
W_{00}^{(1)} &= \frac{1}{2m} + \frac{(\mathbf{p} - \mathbf{p}') \cdot \mathbf{q}}{2m(q^0)^2}, \quad W_{0i}^{(1)} = -\frac{(\mathbf{p} - \mathbf{p}' + \mathbf{q})^i}{2mq^0}, \quad W_{i0}^{(1)} = \frac{-\mathbf{q}^i}{2mq^0}, \quad W_{ij}^{(1)} = \frac{\delta^{ij}}{2m}, \\
Y^{(0)} &= \frac{-q^0}{(\mathbf{p}' - \mathbf{p})^2}, \quad Y^{(1)} = \frac{\mathbf{q} \cdot (\mathbf{p} + \mathbf{p}') + ic_F \boldsymbol{\sigma} \cdot [\mathbf{q} \times (\mathbf{p} - \mathbf{p}')]}{2m(\mathbf{p}' - \mathbf{p})^2}, \\
Y^{(2)} &= \frac{c_D q^0}{8m^2} - \frac{c_S i \boldsymbol{\sigma} \cdot (\mathbf{p}' \times \mathbf{p}) q^0}{4m^2(\mathbf{p}' - \mathbf{p})^2}, \\
Z_0^{(0)} &= \frac{1}{(\mathbf{p}' - \mathbf{p})^2}, \quad Z_i^{(0)} = 0, \quad Z_0^{(1)} = 0, \quad Z_i^{(1)} = \frac{-(\mathbf{p} + \mathbf{p}')^i - ic_F [(\mathbf{p} - \mathbf{p}') \times \boldsymbol{\sigma}]^i}{2m(\mathbf{p}' - \mathbf{p})^2}, \\
Z_0^{(2)} &= -\frac{1}{4m^2} \left[ \frac{c_D}{2} - \frac{c_S i \boldsymbol{\sigma} \cdot (\mathbf{p}' \times \mathbf{p})}{(\mathbf{p}' - \mathbf{p})^2} \right], \quad Z_i^{(2)} = 0.
\end{aligned}$$

$W_{\mu\nu}^{(2)}$  is not required for the calculation here. In Eq. (14) we have set  $\mathbf{p}^2 = \mathbf{p}'^2$ , since this case is sufficient for our analysis. One could also set  $q^0 = |\mathbf{q}|$ , however for calculational purposes we found it simpler to keep factors of  $q^0$  explicit and ignore the energy poles this generates on the real axis.

The coefficients of operators in the soft effective Lagrangian can run. In the soft regime the offshell quark propagators are identical to the quark propagators in heavy quark effective theory (HQET) [10,11]. Therefore, the divergence structure in the soft regime is the same as HQET. The running of  $\mathcal{L}_s$  can be computed indirectly using known results for the HQET Lagrangian,

$$\mathcal{L}_{\text{HQET}} = \psi^\dagger \left\{ iD^0 + \frac{\mathbf{D}^2}{2m} + \frac{c_F g}{2m} \boldsymbol{\sigma} \cdot \mathbf{B} + \frac{c_D g}{8m^2} [\mathbf{D} \cdot \mathbf{E}] + \frac{ic_S g}{8m^2} \boldsymbol{\sigma} \cdot (\mathbf{D} \times \mathbf{E} - \mathbf{E} \times \mathbf{D}) \right\} \psi. \quad (15)$$

The soft Lagrangian at  $\mu = m\nu$  can be computed by first scaling the HQET Lagrangian to  $\mu = m\nu$ , and then matching to the soft Lagrangian by computing the Compton scattering amplitude using HQET vertices in Fig. 2a,b,c. This gives the  $c_F$ ,  $c_D$  and  $c_S$  dependence in Eq. (14). The running coefficients  $c_F$ ,  $c_D$ , and  $c_S$  were computed in Refs. [21–24]:

$$\begin{aligned}
c_F(\nu) &= z^{-C_A/\beta_0}, \quad c_S(\nu) = 2z^{-C_A/\beta_0} - 1, \\
c_D(\nu) &= z^{-2C_A/\beta_0} + \left( \frac{20}{13} + \frac{32C_F}{13C_A} \right) \left[ 1 - z^{-13C_A/(6\beta_0)} \right].
\end{aligned} \quad (16)$$

Here  $z = \alpha_s(m\nu)/\alpha_s(m)$  and  $\beta_0 = 11C_A/3 - 4T_F n_f/3$ , where  $T_F = 1/2$  is the index of the fermion representation.

The renormalization group equation for the potential is

$$\mu \frac{d}{d\mu} \begin{bmatrix} V_{1\otimes 1} \\ V_{T\otimes T} \end{bmatrix} = \frac{\alpha_s}{\pi} \Gamma \begin{bmatrix} V_{1\otimes 1} \\ V_{T\otimes T} \end{bmatrix}, \quad (17)$$

where  $\Gamma$  is a  $2 \times 2$  matrix and can be calculated as a power series in  $v$  and  $\alpha_s$ . The one-loop ultrasoft contributions to  $\Gamma$  are straightforward to compute. Assume that the potential has the form

$$V = (X^A \otimes \bar{X}^A) V(\mathbf{p}, \mathbf{p}'), \quad (18)$$

where  $X^A$  is either  $T^A$  or 1. An ultrasoft loop integrates over the ultrasoft loop-momentum, and due to the multipole expansion does not involve the labels  $\mathbf{p}$  and  $\mathbf{p}'$ , so one can compute all one-loop divergent graphs with a single insertion of  $V$ . In Feynman gauge, the leading order graphs involve the ultrasoft vertex from the  $D^0$  term in  $\mathcal{L}_u$ . The sum of all the graphs has no ultraviolet divergence, so there is no order  $v^0$  ultrasoft contribution to  $\Gamma$  [16]. Thus, the running of the quark potential involves mixing between different powers of  $v$ , i.e. running of the  $v^2$  term proportional to the  $v^0$  term. To the order we are working, we need the ultrasoft vertices from the  $\mathbf{p} \cdot \mathbf{A}/m$  operator, and insertions of  $\mathbf{p} \cdot \nabla/m$ . Graphs with one insertion of  $\nabla^2/(2m)$  or  $\mathbf{p}^4/(8m^3)$  are the same order in the power counting but do not have ultraviolet log divergences. Graphs with one insertion of the operator in Eq. (12) and one  $\mathbf{p} \cdot \mathbf{A}/m$  vertex also do not contribute for this reason. The graphs which contribute to this mixing are listed in Table I and give

$$\Gamma^{(us)} = \frac{2}{3m^2} \begin{bmatrix} C_F \mathbf{k}^2 & -C_1 \mathbf{k}^2 \\ -\mathbf{k}^2 & (C_F + \frac{1}{4}C_d - \frac{3}{4}C_A)\mathbf{k}^2 + C_A(\mathbf{p}^2 + \mathbf{p}'^2) \end{bmatrix}, \quad (19)$$

where

$$C_1 = \frac{N_c^2 - 1}{4N_c^2} = \frac{C_F T_F}{\dim_F}, \quad d^{ABC} d^{ABD} = C_d \delta^{CD}, \quad (20)$$

so  $C_d = (N_c - 4/N_c)$ . Here  $\dim_F$  is the dimension of the fermion representation. In the VRG method introduced in Ref. [16], the scale  $\mu$  in ultrasoft loops is  $m\nu^2$ , and the ultrasoft coupling constant is  $\alpha_s(m\nu^2)$ . Therefore, the ultrasoft contribution to Eq. (17) can be written as

$$\nu \frac{d}{d\nu} \begin{bmatrix} V_{1\otimes 1} \\ V_{T\otimes T} \end{bmatrix} = \frac{2\alpha_s(m\nu^2)}{\pi} \Gamma^{(us)} \begin{bmatrix} V_{1\otimes 1} \\ V_{T\otimes T} \end{bmatrix}. \quad (21)$$

From Eqs. (19) and (21) we see that the Coulomb potential induces running in  $\mathcal{V}_2^{(1)}$ ,  $\mathcal{V}_2^{(T)}$ , and  $\mathcal{V}_r^{(T)}$  proportional to  $\mathcal{V}_c^{(T)}$ .

In addition to the ultrasoft loops, one has the soft contribution shown in Fig. 3. For the soft gluon loops all the infrared divergences are converted to ultraviolet divergences by tadpole diagrams, so with dimensional regularization all  $1/\epsilon$  poles contribute to the anomalous dimensions. The divergent parts of the soft gluon, ghost, and quark loops in Fig. 3 give the running

$$\mu \frac{d}{d\mu} \begin{bmatrix} V_{1\otimes 1} \\ V_{T\otimes T} \end{bmatrix} = \alpha_s^2 \begin{bmatrix} B_{1\otimes 1} \\ B_{T\otimes T} \end{bmatrix}, \quad (22)$$

where for  $n_f$  massless quarks we find

$$B_{1\otimes 1} = \frac{14}{3m^2} C_1, \quad (23)$$

TABLE I. Ultrasoft contributions to the running of the potential in Feynman gauge. The dot denotes an insertion of the potential in Eq. (18). The  $\mathbf{p} \cdot \mathbf{A}$  column gives the momentum factor from diagrams where the gluon coupling is due to the  $\mathbf{p} \cdot \mathbf{A}$  interaction in the Lagrangian. The  $\mathbf{p} \cdot \nabla$  column gives the factor from graphs in which the gluon vertices are from the  $D^0$  interaction, and there are two insertions of the  $\mathbf{p} \cdot \nabla$  operator on the quark lines in the loop. In  $d = 4 - 2\epsilon$  dimensions the ultraviolet divergent part of a diagram is  $-iV(\mathbf{p}, \mathbf{p}')\alpha_s/(2\pi\epsilon m^2)$  times the color and momentum factors. The sum of diagrams is gauge independent.

Diagram	Color Factor	$\mathbf{p} \cdot \mathbf{A}$	$\mathbf{p} \cdot \nabla$
	$T^b X^a T^b \otimes \bar{X}^a$	$\mathbf{p} \cdot \mathbf{p}'$	$-\frac{1}{3}(\mathbf{p}^2 + \mathbf{p}'^2 + \mathbf{p} \cdot \mathbf{p}')$
	$X^a \otimes \bar{T}^b \bar{X}^a \bar{T}^b$	$\mathbf{p} \cdot \mathbf{p}'$	$-\frac{1}{3}(\mathbf{p}^2 + \mathbf{p}'^2 + \mathbf{p} \cdot \mathbf{p}')$
	$T^b X^a \otimes \bar{T}^b \bar{X}^a$	$\mathbf{p}'^2$	$\frac{1}{3}\mathbf{p}'^2$
	$X^a T^b \otimes \bar{X}^a \bar{T}^b$	$\mathbf{p}^2$	$\frac{1}{3}\mathbf{p}^2$
	$T^b X^a \otimes \bar{X}^a \bar{T}^b$	$-\mathbf{p} \cdot \mathbf{p}'$	$-\frac{1}{3}(\mathbf{p}^2 + \mathbf{p}'^2 - \mathbf{p} \cdot \mathbf{p}')$
	$X^a T^b \otimes \bar{T}^b \bar{X}^a$	$-\mathbf{p} \cdot \mathbf{p}'$	$-\frac{1}{3}(\mathbf{p}^2 + \mathbf{p}'^2 - \mathbf{p} \cdot \mathbf{p}')$
	$C_F X^a \otimes \bar{X}^a$	$-(\mathbf{p}^2 + \mathbf{p}'^2)$	$\mathbf{p}^2 + \mathbf{p}'^2$



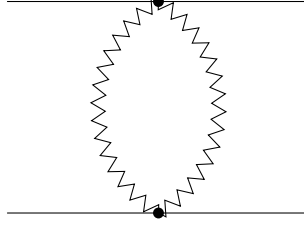


FIG. 3. Soft contributions to the running of the potential. The loop includes soft gluons, ghosts, and massless quarks. Graphs with two  $\sigma = 0$  vertices from Eq. (13) gives the running of the coefficient  $\mathcal{V}_c^{(T)}$ . Graphs with one  $\sigma = 0$  and one  $\sigma = 1$  vertex vanish, while those with one  $\sigma = 0$  and one  $\sigma = 2$ , or two  $\sigma = 1$  vertices contribute to the running of the order  $v^2$  corrections to the potential.

$$\begin{aligned}
B_{T\otimes T} = & -\frac{7}{6m^2}C_d + C_A \left\{ -\frac{22}{3\mathbf{k}^2} + \frac{(39 + 4c_F^2)}{6m^2} - \frac{19(\mathbf{p}^2 + \mathbf{p}'^2)}{3m^2\mathbf{k}^2} + \frac{(11c_S + 10c_F)}{3m^2}\Lambda(\mathbf{p}', \mathbf{p}) \right. \\
& + \frac{c_F^2}{9m^2}\mathbf{S}^2 + \frac{5c_F^2}{18m^2}T(\mathbf{k}) \left. \right\} + \frac{8T_F n_f}{3} \left\{ \frac{1}{\mathbf{k}^2} + \frac{(2c_F^2 - c_D - 1)}{4m^2} + \frac{(\mathbf{p}^2 + \mathbf{p}'^2)}{2m^2\mathbf{k}^2} \right. \\
& \left. - \frac{(c_S + 2c_F)}{2m^2}\Lambda(\mathbf{p}', \mathbf{p}) - \frac{c_F^2}{3m^2}\mathbf{S}^2 - \frac{c_F^2}{12m^2}T(\mathbf{k}) \right\}.
\end{aligned}$$

Here  $B_{1\otimes 1}$  and  $B_{T\otimes T}$  depend on the scale  $\mu = m\nu$  through their dependence on  $c_F$ ,  $c_D$ , and  $c_S$ . In the VRG, the soft coupling constant is  $\alpha_s(m\nu)$ , so the soft contribution to the running is

$$\nu \frac{d}{d\nu} \begin{bmatrix} V_{1\otimes 1} \\ V_{T\otimes T} \end{bmatrix} = \alpha_s^2(m\nu) \begin{bmatrix} B_{1\otimes 1}(m\nu) \\ B_{T\otimes T}(m\nu) \end{bmatrix}. \quad (24)$$

The total VRG running of the potential is given by adding Eqs. (21) and (24). The running of the Coulomb potential is proportional to the beta function,

$$\nu \frac{\partial}{\partial \nu} \mathcal{V}_c^{(T)} = -2\beta_0 \alpha_s^2(m\nu). \quad (25)$$

Integrating Eq. (25) and using the boundary condition in Eq. (7) gives the solution

$$\mathcal{V}_c(\nu) = 4\pi\alpha_s(m\nu), \quad (26)$$

and large logarithms can be avoided by choosing  $\nu = |\mathbf{k}|/m$ . This gives the expected result that the renormalization group improved Coulomb potential is given by choosing  $\alpha_s = \alpha_s(|\mathbf{k}|)$ .

Order  $v$  corrections to the potential such as the one in Eq. (11) do not run at one-loop. The non-trivial result is the renormalization group equations for the order  $v^2$  terms in the potential. Combining Eqs. (21), (24), and using (26) we find

$$\begin{aligned}
\nu \frac{\partial}{\partial \nu} \mathcal{V}_r^{(T)} &= -2(\beta_0 + \frac{8}{3}C_A) \alpha_s^2(m\nu) + \frac{32}{3}C_A \alpha_s(m\nu) \alpha_s(m\nu^2), \\
\nu \frac{\partial}{\partial \nu} \mathcal{V}_2^{(T)} &= \left\{ \frac{1}{2}\beta_0 [1 + c_D(\nu) - 2c_F^2(\nu)] + \frac{1}{6}C_A [28 - 11c_D(\nu) + 26c_F(\nu)^2] - \frac{7}{6}C_d \right\} \alpha_s^2(m\nu) \\
&\quad + \frac{4}{3}(4C_F + C_d - 3C_A) \alpha_s(m\nu) \alpha_s(m\nu^2), \\
\nu \frac{\partial}{\partial \nu} \mathcal{V}_2^{(1)} &= \frac{14}{3}C_1 \alpha_s^2(m\nu) - \frac{16}{3}C_1 \alpha_s(m\nu) \alpha_s(m\nu^2), \\
\nu \frac{\partial}{\partial \nu} \mathcal{V}_s^{(T)} &= \frac{1}{3}(2\beta_0 - 7C_A) c_F^2(\nu) \alpha_s^2(m\nu), \\
\nu \frac{\partial}{\partial \nu} \mathcal{V}_t^{(T)} &= \frac{1}{6}(\beta_0 - 2C_A) c_F^2(\nu) \alpha_s^2(m\nu), \\
\nu \frac{\partial}{\partial \nu} \mathcal{V}_\Lambda^{(T)} &= \left\{ \beta_0 [c_S(\nu) + 2c_F(\nu)] - 4C_A c_F(\nu) \right\} \alpha_s^2(m\nu). \tag{27}
\end{aligned}$$

Note that the soft contributions to the running depend on  $\alpha_s^2(m\nu)$ , and the ultrasoft contributions to the running depend on  $\alpha_s(m\nu) \alpha_s(m\nu^2)$ . This is because the soft gluon coupling is  $g(m\nu)$ , and the ultrasoft gluon coupling is  $g(m\nu^2)$ . The ultrasoft gluon couples via a multipole-expanded interaction, so the ultrasoft interaction vertex does not involve momentum transfers of order  $m\nu$ .

Our results can be checked by comparing with the one-loop formula for the color singlet quark potential in Ref. [18]. The nonrelativistic expansion of the QCD calculation has  $\ln(|\mathbf{k}|/m)$ ,  $\ln(\mu/m)$ , and  $\ln(\lambda/m)$  terms, where a finite gluon mass  $\lambda$  was introduced as an infrared regulator. By explicit computation of the box and crossed box diagrams [25,26] we found that the spin independent potential in Eq. (19) of Ref. [18] is missing the order  $v^2$  term<sup>2</sup>

$$-\frac{4}{3}C_F C_A \alpha_s^2 \frac{(\mathbf{p} + \mathbf{p}')^2}{m^2 \mathbf{k}^2} \ln \left( \frac{\lambda}{|\mathbf{k}|} \right). \tag{28}$$

The  $\ln(|\mathbf{k}|)$  and  $\ln(\lambda)$  dependence in the full theory should be reproduced by the effective theory, so with  $\mu = m$  all QCD logs should be reproduced. We find that the  $\log(\lambda/m)$  terms are reproduced by the ultrasoft diagrams in Table I and that the  $\log(|\mathbf{k}|/m)$  terms are reproduced by the soft loops in Fig. 3.

Solving the VRG equations in Eq. (27) with the tree level boundary conditions in Eq. (7) gives<sup>3</sup>

---

<sup>2</sup>Note that in the calculation in Ref. [17] an expansion was made in  $(\mathbf{p} + \mathbf{p}')^2/\mathbf{k}^2$ , so that the term in Eq. (28) was dropped.

<sup>3</sup>In NRQED the results are simpler since the coupling in the effective theory does not run.

$$\begin{aligned}
\mathcal{V}_r^{(T)}(\nu) &= 4\pi \alpha_s(m\nu) - \frac{16C_A}{3} \alpha_s(m\nu) \alpha_s(m) \ln\left(\frac{m\nu}{m}\right) + \frac{64\pi C_A}{3\beta_0} \alpha_s(m) \ln\left[\frac{\alpha_s(m\nu)}{\alpha_s(m\nu^2)}\right], \\
\mathcal{V}_2^{(T)}(\nu) &= \frac{\pi \left[ C_A(352C_F + 91C_d - 144C_A) - 3\beta_0(33C_A + 32C_F) \right]}{39\beta_0 C_A} \left[ \alpha_s(m\nu) - \alpha_s(m) \right] \\
&\quad + \frac{8\pi(3\beta_0 - 11C_A)(5C_A + 8C_F)\alpha_s(m)}{13C_A(6\beta_0 - 13C_A)} \left[ z^{(1-13C_A/(6\beta_0))} - 1 \right] \\
&\quad + \frac{\pi(\beta_0 - 5C_A)\alpha_s(m)}{(\beta_0 - 2C_A)} \left[ z^{(1-2C_A/\beta_0)} - 1 \right] + \frac{8\pi(4C_F + C_d - 3C_A)}{3\beta_0} \alpha_s(m) \ln\left[\frac{\alpha_s(m\nu)}{\alpha_s(m\nu^2)}\right], \\
\mathcal{V}_2^{(1)}(\nu) &= \frac{14C_1}{3} \alpha_s(m\nu) \alpha_s(m) \ln\left(\frac{m\nu}{m}\right) - \frac{32\pi C_1}{3\beta_0} \alpha_s(m) \ln\left[\frac{\alpha_s(m\nu)}{\alpha_s(m\nu^2)}\right], \\
\mathcal{V}_s^{(T)}(\nu) &= \frac{2\pi\alpha_s(m)}{(2C_A - \beta_0)} \left[ C_A + \frac{1}{3}(2\beta_0 - 7C_A) z^{(1-2C_A/\beta_0)} \right], \\
\mathcal{V}_s^{(1)}(\nu) &= 0, \\
\mathcal{V}_t^{(T)}(\nu) &= -\frac{\pi\alpha_s(m)}{3} z^{(1-2C_A/\beta_0)}, \\
\mathcal{V}_\Lambda^{(T)}(\nu) &= 2\pi\alpha_s(m) \left[ z - 4 z^{(1-C_A/\beta_0)} \right], \tag{29}
\end{aligned}$$

where  $z = \alpha_s(m\nu)/\alpha_s(m)$ . The annihilation contributions can be accounted for by adding the expressions in Eq. (8) to Eq. (29).

The logarithmic corrections to the coefficients in the quark potential were considered by Brambilla et al. [19] using pNRQCD, but were not resummed. Since only the leading perturbative logarithms were included, we can compare our results to theirs by expanding the resummed logarithms in Eq. (29). Brambilla et al. give expressions for the  $\mathcal{V}$ 's in the color singlet channel containing terms of the form

$$\alpha_s(r), \quad \alpha_s \alpha_s(r) \ln(mr), \quad \alpha_s \alpha_s(r) \ln(\mu r). \tag{30}$$

For the soft contributions letting  $\alpha_s(r) \rightarrow \alpha_s(m\nu)$  and  $\ln(r) \rightarrow \ln(1/m\nu)$  in Ref. [19] gives agreement<sup>4</sup> with expanding the soft contributions in Eq. (29) about  $z = 1$  (recalling that  $z = 1 - \beta_0/(2\pi)\alpha_s(m\nu) \ln(m\nu/m)$ ). For the ultrasoft contributions letting  $\ln(\mu/m) \rightarrow \ln(m\nu^2/m)$  in Ref. [19] gives agreement with the ultrasoft contributions in Eq. (29) with the expansion

$$\ln\left[\frac{\alpha_s(m\nu)}{\alpha_s(m\nu^2)}\right] = \frac{\beta_0}{2\pi} \alpha(m\nu) \ln\left(\frac{m\nu^2}{m\nu}\right) + \dots = \frac{\beta_0}{4\pi} \alpha(m\nu) \ln\left(\frac{m\nu^2}{m}\right) + \dots \tag{31}$$

It would be interesting to compare our resummed coefficients to the analogous results computed in pNRQCD. Recall that there is an important distinction between pNRQCD and vNRQCD. In pNRQCD the scales  $m\nu$  and  $m\nu^2$  are treated independently, while vNRQCD builds in the fact that the scales  $m\nu$  and  $m\nu^2$  are not independent. Thus, in vNRQCD, the

---

<sup>4</sup>When comparing the expansion of the color singlet combination  $\mathcal{V}_2^{(1)} - C_F \mathcal{V}_2^{(T)}$  the replacements  $C_d \rightarrow 8C_F - 3C_A$  and  $C_1 \rightarrow C_F C_A/2 - C_F^2$  are also necessary to obtain agreement.

scaling of soft terms from  $m$  to  $mv$ , and ultrasoft terms from  $m$  to  $mv^2$ , occurs simultaneously, and  $\ln(mv)$  and  $\ln(mv^2)$  terms are resummed together.

To see the effect of the running on the value of the coefficients in the potential, consider the case of top quark production near threshold. Projecting onto the color singlet channel gives the singlet coefficients  $\mathcal{V}_i^{(s)} = \mathcal{V}_i^{(1)} - C_F \mathcal{V}_i^{(T)}$ . Using  $\alpha_s(m_t) = 0.108$ , the tree level values in Eq. (7) are:

$$\mathcal{V}_r^{(s)} = -1.81, \quad \mathcal{V}_2^{(s)} = 0, \quad \mathcal{V}_s^{(s)} = 0.60, \quad \mathcal{V}_\Lambda^{(s)} = 0.15, \quad \mathcal{V}_t^{(s)} = 2.71. \quad (32)$$

For a Coulombic system the velocity  $v$  is determined by solving  $\alpha_s(mv) = v$ . Using  $m_t = 175 \text{ GeV}$  and the one-loop running of  $\alpha_s(\mu)$  with  $n_f = 5$  gives  $v = 0.145$ . For  $\nu = v$  the running coefficients in Eq. (29) are:

$$\mathcal{V}_r^{(s)} = -1.49, \quad \mathcal{V}_2^{(s)} = 0.63, \quad \mathcal{V}_s^{(s)} = 0.53, \quad \mathcal{V}_\Lambda^{(s)} = 0.16, \quad \mathcal{V}_t^{(s)} = 3.11. \quad (33)$$

The most substantial change is to the value of  $\mathcal{V}_2^{(s)}$  which was zero at tree level. Using the results of Brambilla et al. with  $mr = 1/v$  and  $\mu = mv^2$  gives

$$\mathcal{V}_r^{(s)} = -1.78, \quad \mathcal{V}_2^{(s)} = 0.68, \quad \mathcal{V}_s^{(s)} = 0.53, \quad \mathcal{V}_\Lambda^{(s)} = 0.16, \quad \mathcal{V}_t^{(s)} = 3.15, \quad (34)$$

indicating that resummation of the logarithms has the largest effect on  $\mathcal{V}_r^{(s)}$ . For the remaining coefficients the resummed values in Eq. (33) are fairly close to the coefficients with perturbative logarithms in Eq. (34).

We would like to thank M. Luke, A. Pineda, and I. Rothstein for helpful discussions. This work was supported in part by the Department of Energy under grant DOE-FG03-97ER40546.

## REFERENCES

- [1] W.E. Caswell and G.P. Lepage, Phys. Lett. **167B**, 437 (1986).
- [2] G.T. Bodwin, E. Braaten and G.P. Lepage, Phys. Rev. **D51**, 1125 (1995), Erratum *ibid.* **D55**, 5853 (1997).
- [3] P. Labelle, Phys. Rev. **D58**, 093013 (1998).
- [4] M. Luke and A.V. Manohar, Phys. Rev. **D55**, 4129 (1997).
- [5] A.V. Manohar, Phys. Rev. **D56**, 230 (1997).
- [6] B. Grinstein and I.Z. Rothstein, Phys. Rev. **D57**, 78 (1998).
- [7] M. Luke and M.J. Savage, Phys. Rev. **D57**, 413 (1998).
- [8] A. Pineda and J. Soto, Nucl. Phys. Proc. Suppl. **64**, 428 (1998);
- [9] A. Pineda and J. Soto, Phys. Rev. **D58**, 114011 (1998).
- [10] M. Beneke and V.A. Smirnov, Nucl. Phys. **B522**, 321 (1998).
- [11] H.W. Griesshammer, Phys. Rev. **D58**, 094027 (1998).
- [12] A. Pineda and J. Soto, Phys. Rev. **D59** 016005 (1999).
- [13] B.A. Kniehl and A.A. Penin, hep-ph/9907489.
- [14] M. Peter, Phys. Rev. Lett. **78**, 602 (1997).
- [15] Y. Schröder, Phys. Lett. **B447** 321 (1999).
- [16] M.E. Luke, A.V. Manohar, and I.Z. Rothstein, hep-ph/9910209.
- [17] S.N. Gupta and S.F. Radford, Phys. Rev. **D24**, 2309 (1981).
- [18] S. Titard and F.J. Yndurain, Phys. Rev. **D49**, 6007 (1994).
- [19] N. Brambilla, A. Pineda, J. Soto and A. Vairo, hep-ph/9907240 and hep-ph/9910238.
- [20] M. Luke and A.V. Manohar, Phys. Lett. **B286**, 348 (1992).
- [21] E. Eichten and B. Hill, Phys. Lett. **B243**, 427 (1990).
- [22] A.F. Falk, B. Grinstein and M.E. Luke, Nucl. Phys. **B357**, 185 (1991).
- [23] B. Blok, J.G. Körner, D. Pirjol and J.C. Rojas, Nucl. Phys. **B496**, 358 (1997).
- [24] C. Bauer and A.V. Manohar, Phys. Rev. **D57**, 337 (1998).
- [25] M.L.G. Redhead, Proc. Roy. Soc. **A220** 219 (1953).
- [26] P.V. Nieuwenhuizen, Nucl. Phys. **B28** 429 (1971).